



Year: 2014

Assessing CpG island methylator phenotype, 1p/19q codeletion, and MGMT promoter methylation from epigenome-wide data in the biomarker cohort of the NOA-04 trial

Wiestler, B ; Capper, D ; Hovestadt, V ; Sill, M ; Jones, D T W ; Hartmann, C ; Felsberg, J ; Platten, M ; Feiden, W ; Keyvani, K ; Pfister, S M ; Wiestler, O D ; Meyermann, R ; Reifenberger, G ; Pietsch, T ; von Deimling, A ; Weller, M ; Wick, W

Abstract: **BACKGROUND** Molecular biomarkers including isocitrate dehydrogenase 1 or 2 (IDH1/2) mutation, 1p/19q codeletion, and O(6)-methylguanine-DNA-methyltransferase (MGMT) promoter methylation may improve prognostication and guide treatment decisions for patients with World Health Organization (WHO) anaplastic gliomas. At present, each marker is individually tested by distinct assays. Illumina Infinium HumanMethylation450 BeadChip arrays (HM450) enable the determination of large-scale methylation profiles and genome-wide DNA copy number changes. Algorithms have been developed to detect the glioma CpG island methylator phenotype (G-CIMP) associated with IDH1/2 mutation, 1p/19q codeletion, and MGMT promoter methylation using a single assay. **METHODS** Here, we retrospectively investigated the diagnostic and prognostic performance of these algorithms in comparison to individual marker testing and patient outcome in the biomarker cohort (n = 115 patients) of the NOA-04 trial. **RESULTS** Concordance for IDH and 1p/19q status was very high: In 92% of samples, the HM450 and reference data agreed. In discordant samples, survival analysis by Kaplan-Meier and Cox regression analyses suggested a more accurate assessment of biological phenotype by the HM450 analysis. The HM450-derived MGMT-STP27 model to calculate MGMT promoter methylation probability revealed this aberration in a significantly higher fraction of samples than conventional methylation-specific PCR, with 87 of 91 G-CIMP tumors predicted as MGMT promoter-methylated. Pyrosequencing of discordant samples confirmed the HM450 assessment in 14 of 17 cases. **CONCLUSIONS** G-CIMP and 1p/19q codeletion are reliably detectable by HM450 analysis and are associated with prognosis in the NOA-04 trial. For MGMT, HM450 suggests promoter methylation in the vast majority of G-CIMP tumors, which is supported by pyrosequencing.

DOI: <https://doi.org/10.1093/neuonc/nou138>

Posted at the Zurich Open Repository and Archive, University of Zurich

ZORA URL: <https://doi.org/10.5167/uzh-98105>

Journal Article

Accepted Version

Originally published at:

Wiestler, B; Capper, D; Hovestadt, V; Sill, M; Jones, D T W; Hartmann, C; Felsberg, J; Platten, M; Feiden, W; Keyvani, K; Pfister, S M; Wiestler, O D; Meyermann, R; Reifenberger, G; Pietsch, T; von Deimling, A; Weller, M; Wick, W (2014). Assessing CpG island methylator phenotype, 1p/19q codeletion,

and MGMT promoter methylation from epigenome-wide data in the biomarker cohort of the NOA-04 trial. *Neuro-Oncology*, 16(12):1630-1638.
DOI: <https://doi.org/10.1093/neuonc/nou138>

Assessing CpG island methylator phenotype, 1p/19q codeletion and *MGMT* promoter methylation from epigenome-wide data in the biomarker cohort of the NOA-04 trial

Benedikt Wiestler^{1,4}, David Capper^{2,5}, Volker Hovestadt⁷, Martin Sill⁸, David TW Jones⁹, Christian Hartmann¹¹, Joerg Felsberg^{12,13}, Michael Platten^{1,6}, Wolfgang Feiden¹⁴, Kathy Keyvani¹⁵, Stefan M Pfister^{3,9}, Otmar D Wiestler¹⁰, Richard Meyermann¹⁶, Guido Reifenberger^{12,13}, Thorsten Pietsch¹⁷, Andreas von Deimling^{2,5}, Michael Weller¹⁸, Wolfgang Wick^{1,4*}

Departments of ¹Neurooncology, ²Neuropathology, and ³Pediatric Oncology, Hematology, and Immunology, Heidelberg University Hospital and German Cancer Consortium (DKTK), Clinical Cooperation Units ⁴Neurooncology, ⁵Neuropathology and ⁶Neuroimmunology and Brain Tumor Immunology, Divisions of ⁷Molecular Genetics, ⁸Biostatistics and ⁹Pediatric Neurooncology, German Cancer Research Center (DKFZ), and ¹⁰DKFZ, 69120 Heidelberg; ¹¹Department for Neuropathology, Institute of Pathology, Medical University of Hannover, 30625 Hannover; ¹²Department of Neuropathology, Heinrich-Heine-University and ¹³DKTK, Düsseldorf, 40225 Düsseldorf; ¹⁴Institute for Neuropathology, Saarland University, 66421 Homburg; ¹⁵Institute for Neuropathology, University of Essen Medical School, 45147 Essen; ¹⁶Institute for Neuropathology, University of Tübingen, 72070 Tübingen; ¹⁷Department of Neuropathology, University of Bonn Medical Center, 53105 Bonn, all Germany; ¹⁸Department of Neurology, University Hospital Zurich, Frauenklinikstrasse 26, CH-8091 Zürich, Switzerland

Running Title: Biomarker assessment in NOA04 using the 450k array

*Corresponding Author:

Wolfgang Wick, Department of Neurooncology, Neurology Clinic & National Center for Tumor Diseases, University of Heidelberg and German Cancer Research Center, Im Neuenheimer Feld 400, D-69120 Heidelberg, phone +49 (0)6221 56 7075, fax +49 (0)6221 56 7554, email: wolfgang.wick@med.uni-heidelberg.de

Funding: The work was supported by the German Cancer Aid (Deutsche Krebshilfe, "Molecular classification of anaplastic gliomas in the NOA-04 trial", project 110624) to WW and MW.

Conflict of interest: MP reports on having received consulting and lecture fees from Merck-Serono, Medac and Novartis as well as research support from Merck-Serono and Novartis.

GR has received a research grant from Roche and honoraria for advisory boards from Roche and Merck-Serono.

MW declares associations with the following companies: Antisense Pharma/Insarna, Bayer, MagForce, Merck Serono, MSD, Roche.

WW reports on having received consulting and lecture fees from MSD and Roche, as well as research support from Apogenix, Boehringer Ingelheim, Eli Lilly, MSD, and Roche. He serves on the Steering Committee of the AVAglio and CENTRIC trials and is lead investigator of other trials in glioma.

DC, AvD, MW and WW receive royalties from the invention of the IDH1 R132H antibody

All other authors have no conflict of interest.

ABSTRACT

Background: Molecular biomarkers, including isocitrate dehydrogenase 1 or 2 (*IDH1/2*) mutation, 1p/19q codeletion and *O*⁶-methylguanine-DNA-methyltransferase (*MGMT*) promoter methylation, may improve prognostication and guide treatment decisions in patients with World Health Organization (WHO) anaplastic gliomas. At present, each marker is individually tested by distinct assays. Illumina Infinium® HumanMethylation450 BeadChip arrays (HM450) enable the determination of large-scale methylation profiles and genome-wide DNA copy number changes. Algorithms have been developed to detect the glioma CpG island methylator phenotype (G-CIMP) associated with *IDH1/2* mutation, 1p/19q codeletion and *MGMT* promoter methylation using a single assay.

Methods: Here, we retrospectively investigated the diagnostic and prognostic performance of these algorithms in comparison to individual marker testing and patient outcome in the biomarker cohort (n=115 patients) of the NOA-04 trial.

Results: Concordance for *IDH* and 1p/19q status was very high: In 92% of cases, the HM450 and the reference data agreed. In discordant cases, survival analysis by Kaplan-Meier and Cox regression analyses suggested a more accurate assessment of the biological phenotype by the HM450 analysis. The HM450-derived *MGMT*-STP27 model to calculate *MGMT* promoter methylation probability revealed this aberration in a significantly higher fraction of cases as conventional methylation-specific PCR, with 87/91 G-CIMP tumors predicted as *MGMT* promoter-methylated. Pyrosequencing of discordant cases confirmed the HM450 assessment in 14/17 cases.

Conclusions: G-CIMP and 1p/19q codeletion are reliably detectable by HM450 analysis and associated with prognosis in the NOA-04 trial. For *MGMT*, HM450

suggests promoter methylation in the vast majority of G-CIMP tumors, which is supported by pyrosequencing.

Key words: 450k, G-CIMP, 1p/19q, anaplastic glioma, *MGMT*

INTRODUCTION

In recent years, insights into the biology of malignant gliomas have considerably increased, leading to the identification of several clinically useful biomarkers.¹ In anaplastic astrocytic, oligodendroglial and oligoastrocytic gliomas of World Health Organization (WHO) grade III, three molecular parameters have been established and extensively characterized as either prognostic or predictive biomarkers.

Combined deletion of chromosomal arms 1p and 19q (1p/19q codeletion), a hallmark of oligodendroglial tumors², has emerged as a well-established prognostic marker in gliomas. Initially regarded as prognostic, this chromosomal aberration also predicted response to combined radio-chemotherapy in the long-term follow-up analyses of two large randomized clinical trials of patients with anaplastic oligodendroglial tumors, i.e. EORTC-26951 and RTOG-9402.^{3,4} Both trials consistently showed that mainly patients with 1p/19q codeleted tumors experience a clinically relevant survival benefit from combined treatment with radiotherapy and procarbazine, CCNU and vincristine (PCV). The molecular mechanisms linking 1p/19q codeletion to increased treatment sensitivity, however, are still poorly understood. In 2011, mutations of *CIC* (homolog of the drosophila gene *capicua*) on chromosome 19q and *far-upstream element binding protein 1* (*FUBP1*) on 1p have been identified as potential mechanisms involved in the biology of 1p/19q codeleted gliomas.⁵

Mutations in the *isocitrate dehydrogenase 1* and *2* genes (*IDH1/2*) were first reported in a small fraction of glioblastoma⁶ and have since then been found at a variable incidence in many gliomas, mostly of WHO grade II and III.¹ Over 70% of anaplastic gliomas carry an *IDH* mutation, with higher frequencies in oligodendroglial tumors⁷ and a strong association with 1p/19q codeletion.⁸ *IDH1/2* mutations are associated with the development of a specific epigenetic hypermethylator signature, the glioma CpG island methylator phenotype (G-CIMP).^{9,10} They also appear to originate from a

distinct cell of origin.¹¹ Randomized clinical trials and larger series have demonstrated a prolonged survival for patients with *IDH1/2* mutant anaplastic gliomas.^{3,12,13} However, in most studies *IDH* mutations do not seem to confer benefit from a specific therapy (radio- or chemotherapy) and hence do not yet carry any predictive properties.

Hypermethylation of the *O*-6-methylguanine-DNA methyltransferase (*MGMT*) promoter has been established to predict response to alkylating chemotherapy in glioblastoma.^{14,15} So far, real-time methylation-specific PCR is the only prospectively validated assay for determination of *MGMT* status in glioblastoma.^{16,17} Mechanistically, modulation of alkylator sensitivity is well explained as *MGMT* catalyzes restoration of guanine from *O*-6-methylguanine, a major genomic lesion induced by alkylating agents. In anaplastic gliomas, however, the situation is more complex. Here, *MGMT* promoter methylation has been found to be a positive prognostic marker independent of treatment in non-overlapping series of anaplastic gliomas.^{12,18} A recent publication shed light on this issue, proposing an interaction between *IDH* mutation and *MGMT* methylation where in the presence of an *IDH1/2* mutation, *MGMT* promoter methylation is merely prognostic (independent of treatment), while in *IDH1/2* wild type anaplastic gliomas, *MGMT* methylation specifically predicts benefit from alkylating chemotherapy.¹⁹

Epigenome-wide analysis of DNA methylation patterns has received increasing attention in brain tumor research, deepening our insight into glioma biology and advancing the classification of tumors.^{10,20} Recently, algorithms have been developed which enable the assessment of all three aforementioned biomarkers from Illumina Infinium® HumanMethylation450 (HM450) data.^{10,20,21} Hybridization of tumor DNA to these arrays allows for methylation profiling of 450,000 CpG sites distributed across the human genome as well as genome-wide copy number profiling.^{20,22} Moreover, the

method is suitable for the analysis of routinely processed formalin-fixed and paraffin-embedded (FFPE) tissue samples.²² In the present study, we aimed to assess the reliability and clinical value of HM450-based determination of G-CIMP, 1p/19q codeletion and *MGMT* promoter hypermethylation in the biomarker cohort of the NOA-04 trial. NOA-04 was designed to assess the optimal sequence of radio- and chemotherapy in patients with newly diagnosed anaplastic gliomas.¹² In NOA-04, *IDH1/2* mutations, 1p/19q codeletion and *MGMT* promoter methylation were prospectively centrally assessed and each marker demonstrated prognostic significance. The NOA-04 trial is hence well suited to investigate the diagnostic (and prognostic) accuracy of HM450-based molecular profiling.

METHODS

Patients, evaluations and ethics

The NOA-04 trial (NCT00717210) for patients with newly diagnosed anaplastic gliomas compared the efficacy and safety of initial radiotherapy, followed by chemotherapy (temozolomide or procarbazine, lomustine and vincristine) at progression or occurrence of unacceptable toxicity with the inverse sequence in patients with newly diagnosed anaplastic gliomas. In this trial, both sequences achieved similar results.¹² Median follow-up time was 54 months. All patients consented to exploratory molecular analyses performed with study data and materials. The original phase III trial was approved by the Ethics Committee (EC) at the University of Tuebingen, Germany, and subsequently all local ECs of the participating clinical centers. NOA-04 enrolled patients after written informed consent including future molecular analyses at 39 sites in Germany.

Molecular analyses

IDH1 codon 132 and *IDH2* codon 172 mutations (Sanger sequencing), 1p/19q codeletion (multiplex ligation-dependent probe assay, MLPA) and *MGMT* promoter methylation (methylation-specific PCR, MSP²³) were centrally determined as described previously.^{12,19} For cases with discordance between *IDH* and G-CIMP status, *IDH1*R132H immunohistochemistry²⁴ (in cases where sequencing indicated the presence of an R132H mutation) or DNA re-extraction and re-sequencing of *IDH1* codon 132 and *IDH2* codon 172 was performed as described.¹⁹ *MGMT* pyrosequencing was performed using Qiagen PyroMark (Qiagen, Hilden, Germany) according to the manufacturer's protocol and evaluated as given in Quillien et al.²⁵ *TERT* promoter mutations (C228 and C250) and ATRX status were previously determined.^{26,27}

DNA extraction and Illumina Infinium® HumanMethylation450 BeadChip array analyses

A tumor cell content of 80% or more was histologically verified prior to DNA extraction for each tumor specimen. For DNA extraction from FFPE tissue samples, the QIAamp DNA Mini Kit (Qiagen, Hilden, Germany) was used. Methylation analysis of 115 samples using the HM450 BeadChip (Illumina, San Diego, CA, USA) was performed at the DKFZ Genomics and Proteomics Core Facility (German Cancer Research Center, Heidelberg, Germany) with normalization to internal controls.

Marker assessment

Unsupervised hierarchical clustering of methylation data was performed as described.²⁰ Briefly, probes (i) with a detection p-value > 0.05, (ii) targeting the X and Y chromosomes, (iii) containing a single nucleotide polymorphism within five base pairs of and including the CpG site and (iv) not mapping uniquely to the human reference genome (hg19), allowing for one mismatch, were removed. The 8000 probes most variable by standard deviation were kept and unsupervised hierarchical clustering was performed.

A logistic regression model to estimate the probability of MGMT promoter methylation from HM450 data was used as described by Bady et al²¹: From the normalized methylated (m) and unmethylated (u) signal intensities, the M-value was calculated: $M\text{-value} = \log_2((m+1)/(u+1))$. The probability of MGMT promoter methylation was calculated as $\text{logit}(y) = 4.3215 + 0.5271 * M\text{-value}(\text{cg12434587}) + 0.9265 * M\text{-value}(\text{cg12981137})$. A probability cut-off at 0.358 was used for scoring unmethylated *versus* methylated.

Copy number aberrations were detected from the HM450 data as described.^{20,22}

Copy number plots were manually analysed for 1p/19q codeletion.

Statistics

Fisher's exact test was used to compare categorical data. To model *MGMT* methylation probability, logistic regression followed by receiver operating characteristic (ROC) curve analysis (using the pROC package²⁸) was employed. For control of the familywise error rate, the Bonferroni procedure was used. Cox proportional hazards regression analysis was performed for survival analysis. A p-value of < 0.05 was considered as statistically significant. All tests were two-sided. Analyses were carried out using R version 3.0.1²⁹ and Stata IC version 12.1 (StataCorp LP, College Station, TX, USA).

RESULTS

Baseline patient characteristics

The present NOA-04 biomarker cohort comprised 115 of the 274 patients of the NOA-04 intention-to-treat (ITT) population, for which tumor DNA of sufficient amount and quality was available. Baseline characteristics of the biomarker cohort and the ITT population were similar (**Table 1**), except for an expected enrichment of patients with resection rather than biopsy because of tissue requirements for this analysis. As in the ITT population, time to treatment failure (TTF), the primary endpoint of the NOA-04 trial, was similar between both arms (log rank $p = 0.94$, **Supplementary Figure 1**). Importantly, in univariate Cox regression analysis, each of the three molecular biomarkers (*IDH1/2* mutation, 1p/19q codeletion and *MGMT* promoter methylation) was significantly associated with survival in the biomarker cohort (**Table 2**).

G-CIMP (as a surrogate for *IDH1/2* mutation) and 1p/19q codeletion status

Unsupervised hierarchical clustering of the normalized HM450-based methylation data identified two main clusters as described previously. Ninety-one of 115 patients (79%) were grouped in the G-CIMP cluster, while 24 patients (21%) belonged to the non-G-CIMP cluster. As expected, presence of *IDH1/2* mutations was strongly associated with the G-CIMP cluster (**Table 3a**, $p < 0.001$, Fisher's exact test). However, in seven patients a G-CIMP phenotype was detected in the absence of an *IDH1/2* mutation. Accordingly, sensitivity and specificity of G-CIMP status for *IDH* mutation were 98% and 72%, respectively. As depicted in the Kaplan-Meier curve in **Figure 1**, the discordant patients (*IDH1/2* wild type, but G-CIMP positive) tended to have a survival more similar to *IDH1/2* mutant / G-CIMP patients rather than *IDH* wild type / Non-G-CIMP patients although no definite conclusions can be drawn because

of the small number of patients. This observation is however substantiated in a Cox regression analysis including both *IDH* and G-CIMP status (**Table 3b**), in which only the G-CIMP status was significantly associated with time to treatment failure. The results for progression-free survival (PFS) were similar (data not shown), while for overall survival (OS), the small number of events precluded statistical testing. Upon re-assessment of the *IDH* status of these 7 patients by *IDH1R132H* immunohistochemistry or DNA re-extraction and re-sequencing, 6 / 7 cases were indeed *IDH* mutant. Further speaking to a correct assessment of the biological phenotype by the G-CIMP status is the observation that 3 out of these 7 cases had a 1p/19q codeletion, which only occurs in *IDH* mutant tumors.⁸ On the other hand, 2 cases with *IDH* mutation did not show the G-CIMP phenotype. For one of these, enough tissue of sufficient quality (vital tumor content > 80%) to re-extract DNA and re-sequence *IDH1 codon 132* and *IDH2 codon 172* was available: As expected, no mutation was found, confirming that this sample is indeed *IDH* wild type.

Analysis of DNA copy-number data generated from the HM450 data revealed combined deletions of 1p and 19q in 41 of 115 patients (35%, example given in **Figure 2a**). As expected, the frequency of 1p/19q codeletion varied among the histological tumor types: It was rare in anaplastic astrocytoma (1 / 50) but rather common in tumors with at least an oligodendroglial component (25 / 45 oligoastrocytomas and 15 / 20 oligodendrogliomas, $p < 0.001$, Fisher's exact test). Agreement of 1p/19q status between MLPA and HM450 was observed in 91 / 99 cases (**Table 4a**, $p < 0.001$, Fisher's exact test). Sensitivity and specificity of HM450 for detection of 1p/19q codeletion with MLPA set as standard were 84% and 98%, respectively. In 7 cases, the HM450 data did not show 1p/19q codeletion whereas MLPA indicated this lesion. Kaplan-Meier analysis (**Figure 2b**) revealed a similar clinical course for these discordant cases and patients whose tumors lacked the

1p/19q codeletion. Cox regression analysis including 1p/19q status from both techniques corroborated this, as again only 1p/19q status computed from HM450 data was significantly associated with survival (**Table 4b**). An overview of clinical and pathological characteristics of all discordant cases is given in **Supplementary Table 4**.

***MGMT* promoter methylation**

Bady et al. proposed a logistic regression model (MGMT-STP27) to predict *MGMT* promoter methylation status from two CpG sites assayed both by the HM27 and HM450 BeadChips.²¹ Applying this algorithm to the NOA-04 dataset indicated that 99 of 115 patients had a methylated *MGMT* promoter (86%), as opposed to 70 / 108 as assessed by MSP (65%). While the MGMT-STP27 algorithm indicated differential *MGMT* methylation in the Non-G-CIMP patients (**Supplementary Table 1a**), virtually all G-CIMP patients were considered to have a methylated *MGMT* promoter based on the HM450 algorithm (87 / 91). Cox regression analysis including both MSP and MGMT-STP27 status clearly demonstrated a closer association of *MGMT* status as per MGMT-STP27 with survival (**Supplementary Table 5**). Interestingly, the concordance of MGMT between the two assays was different for the histological tumor types with good concordance (15 / 17, 88%) in oligodendrogliomas and worse concordance in astrocytomas (19 / 31, 61%).

Constructing a 95% confidence interval (based on the standard error of the fit) for each prediction resulted in 9 samples to be considered unclassifiable (as the confidence interval for methylation probability crossed the cut-off). To improve the prediction model for *MGMT* promoter methylation in the G-CIMP-positive tumors, we re-evaluated the 18 CpG sites within the *MGMT* 5'-CpG island originally investigated by Bady et al. in our cohort of 88 patients with G-CIMP positive tumors with known

MGMT promoter methylation status determined by MSP analysis. After Bonferroni adjustment to correct for type-I-error inflation, five CpG probes were significantly associated (as per univariate logistic regression) with *MGMT* methylation probability (**Supplementary Table 2**). Notably, this group contained both probes (cg12434587 & cg12981137) included in the *MGMT*-STP27 model. The remaining probes are located nearby to either of these two probes (**Supplementary Figure 2**). In a next step, we stepwise built prediction models from these probes. To limit overfitting, we used Akaike's information criterion (AIC) with the default parameter ($k = 2$) for factor penalization. This approach yielded two models with similar AUC and AIC values (**Table 5**), one of them being the *MGMT*-STP27 (albeit with different regression coefficients and cut point). The ROC curves are shown in **Figure 3**, **Supplementary Table 3** lists the predicted *MGMT* promoter methylation status for both models. Given the limited diagnostic accuracy of both models, *MGMT* methylation status as calculated from any of these two models was not significantly associated with outcome (**Supplementary Table 3**). To resolve the discrepancy between the *MGMT*-STP27 and MSP findings, we performed *MGMT* pyrosequencing on all 17 discordant G-CIMP cases (methylated per *MGMT*-STP27, unmethylated per MSP), for which enough DNA of sufficient quality was left: Using a pre-defined mean methylation of 8% as cut-off²⁵, 14 samples were classified as *MGMT* methylated and only 3 as *MGMT* unmethylated.

Relationship between *IDH1/2* mutation/G-CIMP, 1p/19q codeletion and *MGMT* promoter methylation

In this series, 93% (43 / 46) of all tumors with a 1p/19q codeletion (MLPA) carried an *IDH* mutation. Considering the HM450 data, all 41 samples with 1p/19q codeletion clustered in the G-CIMP group. Almost all 1p/19q codeleted tumors (HM450)

displayed a methylated *MGMT* promoter (37 / 41). In general, the frequency of *MGMT* promoter hypermethylation was higher in tumors with an *IDH* mutation: 73% (61 / 83) of tumors with an *IDH1/2* mutation, as opposed to 36% (9 / 25) of the *IDH1/2* wild type tumors had *MGMT* promoter methylation (see also¹⁹). For G-CIMP, 1p/19q and *MGMT* (all assessed *via* the HM450), Cox regression demonstrated a prognostic impact independent of reference histology (**Supplementary Table 6**).

DISCUSSION

For optimal management of patients with anaplastic gliomas, there is clinical need for reliable information on 1p/19q, *IDH1/2* and *MGMT* status.³⁰ Thus, molecular testing for these markers is increasingly being requested in neurooncology. Additional information derived from genome-wide analyses may be valuable, both for molecular subgrouping of tumors^{10,31} and identification of novel therapeutic targets.³² The Illumina Infinium® HumanMethylation450 BeadChip array platform, which has been shown to separate glioblastoma into six biologically meaningful molecular subgroups²⁰, allows for the simultaneous assessment of these three most relevant biomarkers in anaplastic gliomas and additionally provides a powerful tool for future discoveries. In the present study, we have evaluated the diagnostic and prognostic reliability of biomarker assessment based on the HM450 array in a subgroup of patients of the NOA-04 trial and thus asked whether this technology - where available - may replace separate single marker testing. While G-CIMP and 1p/19q status were determined concordantly to the single marker tests, *MGMT* promoter methylation assessment differed considerably between MSP and the HM450-derived algorithm, especially in the G-CIMP tumors. Here, pyrosequencing of discordant cases suggested that most G-CIMP anaplastic glioma in fact carry a methylated *MGMT* promoter, as suggested by the HM450.

For determination of *IDH1/2* mutation, 1p/19q codeletion and *MGMT* promoter methylation status, a plethora of diagnostic methods exist without a uniformly agreed-upon “gold standard”. Tissue requirements (both source and amount) as well as costs for testing constitute further issues to be considered. For the assessment of *IDH* mutation, sequencing of *IDH1* codon 132 and *IDH2* codon 172 as well as immunohistochemistry targeted against *IDH1R132H* are the most commonly used methods.³³ While immunohistochemistry is a well-established technique with minimal

tissue requirements, it misses the (albeit rare) *IDH* mutations other than *IDH1R132H*.²⁴ Sequencing, on the other hand, may miss low-level mutations. Fluorescence *in situ* hybridization (FISH) is nowadays probably the most commonly used assay to determine the 1p/19q status.³⁴ It can easily be performed without the need for DNA extraction and hence avoiding dilution by normal cells. However, most commercially available probes are not able to distinguish partial and total deletions. Two smaller series have demonstrated a strong correlation between 1p/19q status as assessed by FISH and MLPA.^{35,36} For determination of the *MGMT* promoter methylation status, even a larger number of distinct diagnostic assays do exist, including MSP, pyrosequencing, methylation-sensitive high-resolution melting or MethyLight, and others.³⁷ The original report of the predictive value of *MGMT* methylation in glioblastoma was performed using MSP.¹⁴ To date, real-time MSP is the only prospectively validated test for *MGMT* promoter methylation assessment in glioblastoma.¹⁶ However, an internationally accepted consensus about the most appropriate diagnostic method to be used for *MGMT* testing is still missing. Unfortunately, most other methodologies lack published validation according to guidelines for molecular diagnostics. In practice, the choice of method thus preferentially depends on the individual experience and equipment of each laboratory, e.g. availability of a pyrosequencer or real time PCR machine and the level of validation.

Both for the *IDH1/2* / G-CIMP and 1p/19q status, our comparative analyses of the NOA-04 biomarker cohort revealed only small subsets of cases showing discordant results when tested by HM450 arrays versus individual assays, i.e. *IDH1/2* sequencing and 1p/19q MLPA, respectively. In our series, 7 *IDH1/2* wild type tumors by sequencing of codon 132 and 172, respectively, demonstrated G-CIMP (**Table 3a**), which in part may be false-negative results due to the weak signal in the direct

Sanger sequencing.³³ Consequently, re-examination of these 7 cases revealed that 6 tumors actually carried an *IDH* mutation, as correctly predicted by the HM450 array. Conversely, of 2 cases with *IDH* mutation but without a G-CIMP, 1 case could be re-analyzed and no *IDH* mutation was found, indicating that the initially reported *IDH* mutation was a false-positive result. Considering that *IDH* mutation causes the G-CIMP⁹, this is not surprising and suggests that the other case will probably also be a false-positive *IDH* mutation. Similarly, in the few discordant 1p/19q cases (1p/19q codeleted based on MLPA, 1p/19q intact as per HM450), the clinical course and pathological characteristics tended to accord to the HM450 data (**Figure 2b, Table 4b, Supplementary Table 4**): Four of these 7 discordant cases were classified as anaplastic astrocytoma in reference histology, and of the remaining 3 cases, 1 case was classified as G-CIMP negative. In a previous analysis, we identified 3 cases carrying both ATRX (alpha-thalassemia/mental retardation syndrome X-linked) loss and 1p/19q codeletion, which should be mutually exclusive.²⁷ Of these, 2 had an intact 1p/19q status as per HM450, while the third was not included in this cohort. *TERT* promoter mutations are strongly associated with the presence of 1p/19q codeletion in *IDH* mutant gliomas.³⁸ Further supporting the HM450 1p/19q results, in 6/7 cases where HM450-based 1p/19q analysis indicated no codeletion (while MLPA did), *TERT* promoter status was wild type, while in one case where HM450 indicated 1p/19q codeletion as opposed to MLPA, a *TERT* promoter mutation was found. Taken together, the 1p/19q MLPA assessment of the initial NOA-04 trial likely resulted in a number of misclassified cases and particularly in an overestimation of the rate of 1p/19q codeleted tumors. This may be explained by the rather low threshold chosen in the initial MLPA assessment where two adjacent gene loci with a gene dosage ratio of less than 70% were considered as evidence of chromosome arm deletion.

In anaplastic gliomas, *MGMT* promoter methylation is merely prognostic and not predictive for a benefit from alkylating chemotherapy, most likely due to an interaction with the *IDH1/2* mutation status.¹⁹ The MGMT-STP27 model with a reported AUC of 0.97, a sensitivity of 0.97 and a specificity of 0.89 in G-CIMP negative tumors²¹, predicted *MGMT* promoter methylation in the vast majority of G-CIMP positive tumors (87 / 91) as opposed to the MSP (62 / 88 tumors methylated, three cases missing *MGMT* data). This strong association between *MGMT* methylation and *IDH* mutation has been noted before in the original report by Bady²¹ and is also shown by others using pyrosequencing.³⁹ Cox regression analysis including both MSP and MGMT-STP27 status clearly demonstrated a closer association of *MGMT* status as per MGMT-STP27 with survival (**Supplementary Table 5**). There was a clear association of the discordant *MGMT* assessment with histological subtype (high rates of discordant cases especially in astrocytomas). This may be a result of a lower sensitivity of MSP assessment in the more diffuse astrocytic tumors compared to often more compact oligodendroglial tumors and may also influence survival analysis. Using our cohort of 88 G-CIMP patients with known *MGMT* promoter methylation status as determined by MSP, we tried to build a new *MGMT* prediction model for G-CIMP tumors based on the probes identified by Bady et al.²¹ Malley et al. defined two regions in the *MGMT* CpG island where hypermethylation was significantly associated with reduced *MGMT* mRNA expression (differentially methylated regions, DMR).⁴⁰ Of these, pyrosequencing of DMR2 (chr10:131,265,496 – 131,265,626) demonstrated hypermethylation in almost all adult *IDH* mutant gliomas.³⁹ This region is also covered by the forward and reverse MSP primers used in NOA-04 as well as two of the five cg probes on the HM450 significantly associated with *MGMT* methylation (cg02802904 & cg12981137) (**Supplementary Figure 2**). Importantly, cg12981137 is contained in the MGMT-STP27 model as well as in the two newly-

fitted models. However, the two models for which Akaike's AIC indicated the best fit resulted in an AUC of only 0.84 in ROC analysis (**Table 5** and **Figure 3**). Consequently, both models were not significantly associated with survival (**Supplementary Table 3**). To resolve the discrepancy between the MGMT-STP27 and MSP findings, we performed *MGMT* pyrosequencing on all 17 discordant G-CIMP cases (methylated per MGMT-STP27, unmethylated per MSP) for which enough DNA of sufficient quality was left: Using a pre-defined mean methylation of 8% as cut-off²⁵, 14 samples were classified as *MGMT* methylated and only 3 as *MGMT* unmethylated, further supporting the notion that most *IDH* mutant / G-CIMP anaplastic gliomas carry a methylated *MGMT* promoter.

Due to dense genomic coverage of the HM450, copy number analysis is possible in addition to methylation profiling as demonstrated.²⁰ This allows the identification of multiple important and immediately relevant molecular aberrations¹ using a single array, even retrospectively in archival tissue. Furthermore, while in the original NOA-04 trial, some cases lacked molecular information, mostly 1p/19q status¹², these parameters could be completely assessed for all patients based on the HM450 data. While the reported observations point towards a very good diagnostic and prognostic accuracy of the HM450 data, it is important to note that while this is a prospective, well documented and homogenous trial cohort, this comparison was not pre-specified. Furthermore, the subset of patients investigated here is not necessarily representative for the entire NOA-04 trial cohort (even though the main prognostic factors and the equivalence of both treatment arms are recapitulated) and may be subject to bias, although all patients with sufficient tumor DNA were included.

The HM450 approach thus accurately identified G-CIMP and 1p/19q status in this NOA-04 cohort. In discordant cases, the result from the HM450 data seemed to be clinically more useful as they appeared to better predict patient outcome and were

usually confirmed by reanalysis of discordant cases using different diagnostic tests. In addition to the biomarker information, the HM450 array yields epigenome-wide methylation data, which provide a powerful dataset for future discoveries.^{10,20} For *MGMT* methylation, the HM450 data indicates that most G-CIMP tumors carry a methylated *MGMT* promoter (as opposed to the MSP data), which is supported by other studies and pyrosequencing of the discordant cases. In conclusion, these NOA-04-based results are encouraging. They should be verified in an independent trial, such as EORTC-26951 or CATNON.

ACKNOWLEDGEMENTS

Some of the authors (GR, MW and WW) conducting this work represent the Neurooncology Working Group (NOA) of the German Cancer Society.

We are indebted to the patients and their families for agreeing to participate in the NOA-04 trial, as well as to the study nurses and data managers for their collaboration.

The following institutions and investigators in Germany participated in the trial: Klinikum Aschaffenburg (S Kaendler); Nervenlink, Bamberg, Germany (P Krauseneck); Charité Universitätsmedizin Berlin, Berlin (G Auf, M Kufeld, F Stockhammer); Universitätsklinikum (UK) Düsseldorf, Düsseldorf (M Rapp, MC Sabel); UK Erlangen, Erlangen (I Blümcke, GG Grabenbauer, W Wolf); UK Essen, Essen (P Cicotti, HC Diener, R Egensperger, C Ehrenfeld, KW Schmidt); UK Frankfurt, Frankfurt a. M. (K Franz); UK Giessen-Marburg, Campus Giessen (K Kuchelmeister, U Nestler, M Winking); UK Greifswald, Greifswald (E Asse, M Montemurro); Allgemeines Krankenhaus Hagen, Hagen (G Ansorge, R Souchon); UK Halle-Wittenberg, Halle (C Holz); Henriettenstiftung Krankenhaus Hannover, Hannover (B Wiese); Med. Hochschule; Hannover (CA Tschan); UK Heidelberg, Heidelberg (M Vogt-Schaden); KKH Heidenheim, Heidenheim (D Steder); UK Homburg (R Ketter, WI Steudel); UK Jena, Jena (A Hochstetter); UK Schleswig-Holstein, Campus Kiel (H-H Hugo, M Mehdorn, S Mihajlovic, S Schultka); UK Köln, Köln (G Garlip); Klinikum Ludwigsburg, Ludwigsburg (M Schabet, E Weimann); UK Schleswig-Holstein, Campus Lübeck (AC Feller, T Niehoff, M Nitschke, E Reusche); UK Mainz, Mainz (H Müller, C Sommer, D Wiewrodt); UK Giessen-Marburg, Campus Marburg (R Engenhardt-Cabillic, M Groß); Klinikum Im Mühlenkreis, Minden (F Haukamp); Klinikum Großhadern, München (C Dudel); Klinikum Rechts der Isar,

München (C Nieder, S Reitz); Praxis Hoffmann, Norderstedt (R Hoffmann); Praxis Heide/Thiel, Stade (J Heide, C Thiel); Klinikum Nürnberg, Nürnberg (G Schmidt, K Westphal); Bezirkskrankenhaus Regensburg, Regensburg (U Bogdahn, P Hau, B Hirschmann); Katharinenhospital, Stuttgart (C Seidenberg); UK Tübingen, Tübingen (M Bamberg, U Herrlinger, R Kortmann, R Meyermann, M Platten, F Schmidt, J Steinbach, M Weller, W Wick); Marienhospital, Vechta (J Diers); Kliniken St. Antonius, Velbert (I Blaeser); Städt. Klinik, Zwickau (E Hamann).

We thank Matthias Schick and Roger Fischer from the DKFZ Genomics Core Facility for performing the microarray analyses to a very high standard. The work was supported by the German Cancer Aid (Deutsche Krebshilfe, "Molecular classification of anaplastic gliomas in the NOA-04 trial") to WW and MW.

REFERENCES

1. Weller M, Pfister SM, Wick W, et al. Molecular neuro-oncology in clinical practice: a new horizon. *Lancet Oncol.* 2013;14(9):e370–379.
2. Smith JS, Perry A, Borell TJ, et al. Alterations of chromosome arms 1p and 19q as predictors of survival in oligodendrogliomas, astrocytomas, and mixed oligoastrocytomas. *J. Clin. Oncol.* 2000;18(3):636–645.
3. Van den Bent MJ, Brandes AA, Taphoorn MJB, et al. Adjuvant procarbazine, lomustine, and vincristine chemotherapy in newly diagnosed anaplastic oligodendroglioma: long-term follow-up of EORTC brain tumor group study 26951. *J. Clin. Oncol.* 2013;31(3):344–350.
4. Cairncross G, Wang M, Shaw E, et al. Phase III trial of chemoradiotherapy for anaplastic oligodendroglioma: long-term results of RTOG 9402. *J. Clin. Oncol.* 2013;31(3):337–343.
5. Bettegowda C, Agrawal N, Jiao Y, et al. Mutations in CIC and FUBP1 contribute to human oligodendroglioma. *Science.* 2011;333(6048):1453–1455.
6. Parsons DW, Jones S, Zhang X, et al. An integrated genomic analysis of human glioblastoma multiforme. *Science.* 2008;321(5897):1807–1812.
7. Yan H, Parsons DW, Jin G, et al. IDH1 and IDH2 mutations in gliomas. *N. Engl. J. Med.* 2009;360(8):765–773.
8. Labussière M, Idbaih A, Wang X-W, et al. All the 1p19q codeleted gliomas are mutated on IDH1 or IDH2. *Neurology.* 2010;74(23):1886–1890.
9. Turcan S, Rohle D, Goenka A, et al. IDH1 mutation is sufficient to establish the glioma hypermethylator phenotype. *Nature.* 2012;483(7390):479–483.
10. Nouchmehr H, Weisenberger DJ, Diefes K, et al. Identification of a CpG island methylator phenotype that defines a distinct subgroup of glioma. *Cancer Cell.* 2010;17(5):510–522.
11. Lai A, Kharbanda S, Pope WB, et al. Evidence for sequenced molecular evolution of IDH1 mutant glioblastoma from a distinct cell of origin. *J. Clin. Oncol.* 2011;29(34):4482–4490.
12. Wick W, Hartmann C, Engel C, et al. NOA-04 randomized phase III trial of sequential radiochemotherapy of anaplastic glioma with procarbazine, lomustine, and vincristine or temozolomide. *J. Clin. Oncol.* 2009;27(35):5874–5880.
13. Sanson M, Marie Y, Paris S, et al. Isocitrate dehydrogenase 1 codon 132 mutation is an important prognostic biomarker in gliomas. *J. Clin. Oncol.* 2009;27(25):4150–4154.

14. Hegi ME, Diserens A-C, Gorlia T, et al. MGMT gene silencing and benefit from temozolomide in glioblastoma. *N. Engl. J. Med.* 2005;352(10):997–1003.
15. Wick W, Platten M, Meisner C, et al. Temozolomide chemotherapy alone versus radiotherapy alone for malignant astrocytoma in the elderly: the NOA-08 randomised, phase 3 trial. *Lancet Oncol.* 2012;13(7):707–715.
16. Gilbert MR, Wang M, Aldape KD, et al. Dose-Dense Temozolomide for Newly Diagnosed Glioblastoma: A Randomized Phase III Clinical Trial. *J. Clin. Oncol.* 2013;31(32):4085–4091.
17. Vlassenbroeck I, Califice S, Diserens A-C, et al. Validation of real-time methylation-specific PCR to determine O6-methylguanine-DNA methyltransferase gene promoter methylation in glioma. *J. Mol. Diagnostics.* 2008;10(4):332–337.
18. Van den Bent MJ, Dubbink HJ, Sanson M, et al. MGMT promoter methylation is prognostic but not predictive for outcome to adjuvant PCV chemotherapy in anaplastic oligodendroglial tumors: a report from EORTC Brain Tumor Group Study 26951. *J. Clin. Oncol.* 2009;27(35):5881–5886.
19. Wick W, Meisner C, Hentschel B, et al. Prognostic or predictive value of MGMT promoter methylation in gliomas depends on IDH1 mutation. *Neurology.* 2013;81(17):1515–1522.
20. Sturm D, Witt H, Hovestadt V, et al. Hotspot mutations in H3F3A and IDH1 define distinct epigenetic and biological subgroups of glioblastoma. *Cancer Cell.* 2012;22(4):425–437.
21. Bady P, Sciuscio D, Diserens A-C, et al. MGMT methylation analysis of glioblastoma on the Infinium methylation BeadChip identifies two distinct CpG regions associated with gene silencing and outcome, yielding a prediction model for comparisons across datasets, tumor grades, and CIMP-status. *Acta Neuropathol.* 2012;124(4):547–560.
22. Hovestadt V, Remke M, Kool M, et al. Robust molecular subgrouping and copy-number profiling of medulloblastoma from small amounts of archival tumour material using high-density DNA methylation arrays. *Acta Neuropathol.* 2013;125(6):913–916.
23. Krex D, Klink B, Hartmann C, et al. Long-term survival with glioblastoma multiforme. *Brain.* 2007;130(10):2596–2606.
24. Capper D, Weissert S, Balss J, et al. Characterization of R132H mutation-specific IDH1 antibody binding in brain tumors. *Brain Pathol.* 2010;20(1):245–254.
25. Quillien V, Lavenue A, Karayan-Tapon L, et al. Comparative assessment of 5 methods (methylation-specific PCR, MethyLight, pyrosequencing, methylation-sensitive high-resolution melting, and immunohistochemistry) to analyze O6-

- methylguanine-DNA-methyltransferase in a series of 100 glioblastoma patients. *Cancer*. 2012;118(17):4201–4211.
26. Koelsche C, Sahm F, Capper D, et al. Distribution of TERT promoter mutations in pediatric and adult tumors of the nervous system. *Acta Neuropathol*. 2013;126(6):907–915.
 27. Wiestler B, Capper D, Holland-Letz T, et al. ATRX loss refines the classification of anaplastic gliomas and identifies a subgroup of IDH mutant astrocytic tumors with better prognosis. *Acta Neuropathol*. 2013;126(3):443–451.
 28. Robin X, Turck N, Hainard A, et al. pROC: an open-source package for R and S+ to analyze and compare ROC curves. *BMC Bioinformatics*. 2011;1277.
 29. R Core Team. R: A language and environment for statistical computing. R Foundation for Statistical Computing, Vienna, Austria. ISBN 3-900051-07-0, URL <http://www.R-project.org/>. 2013
 30. Weller M & Wick W. Neuro-oncology in 2013: improving outcome in newly diagnosed malignant glioma. *Nat. Rev. Neurol*. 2014;10(2):68–70.
 31. Verhaak RGW, Hoadley KA, Purdom E, et al. Integrated genomic analysis identifies clinically relevant subtypes of glioblastoma characterized by abnormalities in PDGFRA, IDH1, EGFR, and NF1. *Cancer Cell*. 2010;17(1):98–110.
 32. Frattini V, Trifonov V, Chan JM, et al. The integrated landscape of driver genomic alterations in glioblastoma. *Nat. Genet*. 2013;45(10):1141–1149.
 33. Preusser M, Capper D & Hartmann C. IDH testing in diagnostic neuropathology: review and practical guideline article invited by the Euro-CNS research committee. *Clin. Neuropathol*. 2011;30(5):217–230.
 34. Horbinski C, Miller CR & Perry A. Gone FISHing: clinical lessons learned in brain tumor molecular diagnostics over the last decade. *Brain Pathol*. 2011;21(1):57–73.
 35. Natté R, van Eijk R, Eilers P, et al. Multiplex ligation-dependent probe amplification for the detection of 1p and 19q chromosomal loss in oligodendroglial tumors. *Brain Pathol*. 2005;15(3):192–197.
 36. Franco-Hernández C, Martínez-Glez V, de Campos JM, et al. Allelic status of 1p and 19q in oligodendrogliomas and glioblastomas: multiplex ligation-dependent probe amplification versus loss of heterozygosity. *Cancer Genet. Cytogenet*. 2009;190(2):93–96.
 37. Weller M, Stupp R, Reifenberger G, et al. MGMT promoter methylation in malignant gliomas: ready for personalized medicine? *Nat. Rev. Neurol*. 2010;6(1):39–51.

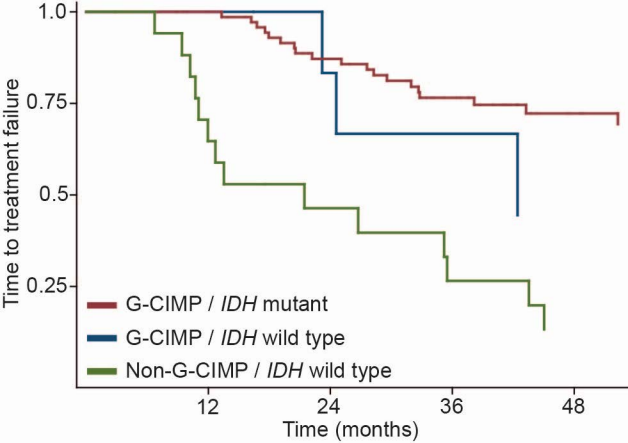
38. Killela PJ, Reitman ZJ, Jiao Y, et al. TERT promoter mutations occur frequently in gliomas and a subset of tumors derived from cells with low rates of self-renewal. *Proc. Natl. Acad. Sci. U. S. A.* 2013;110(15):6021–6026.
39. Mulholland S, Pearson DM, Hamoudi RA, et al. MGMT CpG island is invariably methylated in adult astrocytic and oligodendroglial tumors with IDH1 or IDH2 mutations. *Int. J. Cancer.* 2012;131(5):1104–1113.
40. Malley DS, Hamoudi RA, Kocialkowski S, et al. A distinct region of the MGMT CpG island critical for transcriptional regulation is preferentially methylated in glioblastoma cells and xenografts. *Acta Neuropathol.* 2011;121(5):651–661.

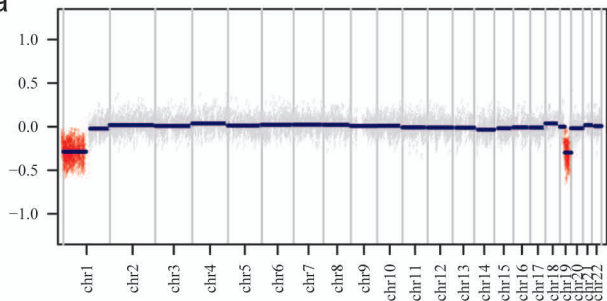
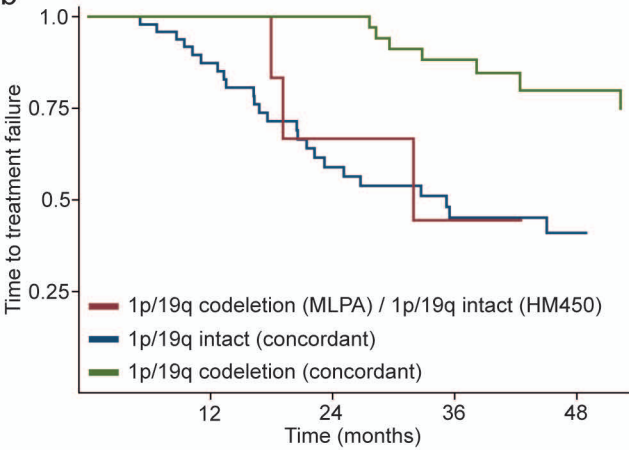
FIGURE LEGENDS

Figure 1: Time to treatment failure by G-CIMP/*IDH* status. The two samples Non-G-CIMP / *IDH* mutant cases were omitted as KM-curves with two patients are not considered informative.

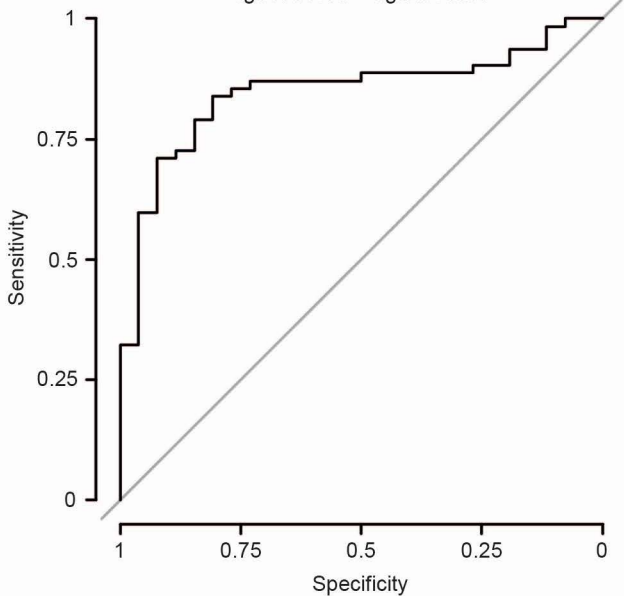
Figure 2: 1p/19q status. (a) Example of a copy number plot generated from HumanMethylation450 data of a patient with 1p/19q codeletion. (b) Kaplan-Meier curve for TTF based on 1p/19q status (assessed by MLPA and HumanMethylation450). The 1 discordant case with 1p/19q codeletion as per HumanMethylation450 and intact 1p/19q status (MLPA) was omitted.

Figure 3: MGMT promoter methylation prediction. ROC curves for the two models with the best fit (as per AIC).



a**b**

cg14194875 + cg12981137



cg12434587 + cg12981137

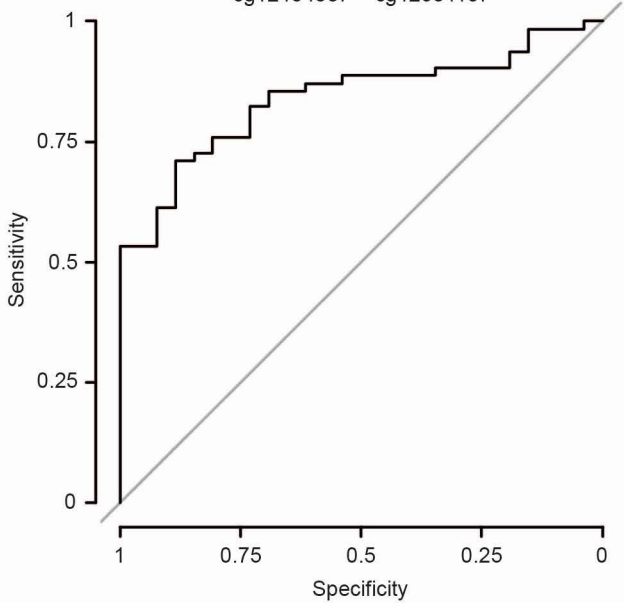


Table 1. Baseline patient characteristics

	NOA-04 Biomarker Cohort		NOA-04 Trial Cohort	
	RT (n = 65)	PCV / TMZ (n = 50)	RT (n = 139)	PCV / TMZ (n = 135)
Median age (range), years	42 (23 – 74)	41.5 (25 – 64)	44 (23 – 74)	42 (20 – 77)
Astrocytoma, n	28 (43%)	22 (43%)	70 (50%)	74 (55%)
Oligoastrocytoma, n	25 (38%)	20 (40%)	47 (34%)	44 (32%)
Oligodendroglioma, n	12 (19%)	8 (17%)	22 (16%)	17 (13%)
Resection, n				
Total	31 (48%)	22 (44%)	53 (38%)	47 (35%)
Subtotal	33 (50.5%)	27 (54%)	61 (44%)	57 (42%)
Biopsy	1 (1.5%)	1 (2%)	25 (18%)	31 (23%)
1p/19q co-deletion, n				
Yes	27 (46%)	19 (46%)	41 (43%)	33 (38%)
No	31 (54%)	22 (54%)	54 (57%)	53 (62%)
Information missing	7	9	44	49
MGMT promoter, n				
Methylated	37 (60%)	33 (70%)	59 (57%)	64 (64%)
Unmethylated	24 (40%)	14 (30%)	44 (43%)	35 (36%)
Information missing	4	3	36	36
IDH mutation, n				
Yes	48 (78%)	35 (74%)	65 (66%)	68 (70%)
No	13 (22%)	12 (26%)	33 (34%)	29 (30%)
Information missing	4	3	41	38

Formatiert: Zeilenabstand: Doppelt

Formatiert: Zeilenabstand: Doppelt

Formatiert: Zeilenabstand: Doppelt

Formatiert: Zeilenabstand: Doppelt

Formatiert: Zeilenabstand: Doppelt

Formatiert: Zeilenabstand: Doppelt

Formatiert: Zeilenabstand: Doppelt

RT, radiotherapy; PCV, procarbazine, CCNU & vincristine; TMZ, temozolomide

Formatiert: Zeilenabstand: Doppelt

|

|

N-O-D-14-00023R1 TABLES -2-

Formatiert: Englisch (USA)

Feldfunktion geändert

Formatiert: Englisch (USA)

Formatiert: Block, Zeilenabstand:
Doppelt

Formatiert: Englisch (USA)

Formatiert: Englisch (USA)

Feldfunktion geändert

Table 2. Univariate Cox regression in the NOA-04 biomarker cohort

Formatiert: Zeilenabstand: Doppelt

Variable	Hazard Ratio	95% CI	p
<i>IDH</i> mutation vs. wild type	0.2	0.1 - 0.37	< 0.001
1p/19q codeletion, yes vs. no	0.26	0.13 - 0.55	< 0.001
<i>MGMT</i> methylated vs. unmethylated	0.5	0.28 - 0.92	0.026

Formatiert: Zeilenabstand: Doppelt

Formatiert: Zeilenabstand: Doppelt

Formatiert: Zeilenabstand: Doppelt

CI, confidence interval; *IDH*, isocitrate dehydrogenase; *MGMT*, *O*⁶-methylguanine-DNA-methyltransferase

Formatiert: Zeilenabstand: Doppelt

Formatiert: Block, Abstand Nach: 0 Pt., Zeilenabstand: Doppelt

Table 3: *IDH* and G-CIMP status as per NOA-04 assessment and HM450.A) Tabulation of *IDH* mutation and G-CIMP status

Formatiert: Zeilenabstand: Doppelt

	G-CIMP	Non-G-CIMP
<i>IDH</i> mutant	81	2
<i>IDH</i> wild type	7	18

Formatiert: Block, Zeilenabstand: Doppelt

Formatiert: Block, Zeilenabstand: Doppelt

Formatiert: Block, Zeilenabstand: Doppelt

Formatiert: Zeilenabstand: Doppelt

B) Cox regression for *IDH* and G-CIMP status

Variable	Hazard Ratio	95% CI	p
<i>IDH</i> mutation vs. wild type	0.45	0.15 - 1.3	0.14
G-CIMP vs. Non-G-CIMP	0.32	0.1 - 0.94	0.038

Formatiert: Zeilenabstand: Doppelt

Formatiert: Zeilenabstand: Doppelt

CI, confidence interval; G-CIMP, glioma CpG island methylator phenotype;

Formatiert: Zeilenabstand: Doppelt

IDH, isocitrate dehydrogenase

Formatiert: Block, Abstand Nach: 0 Pt., Zeilenabstand: Doppelt

Table 4: 1p/19q status by MLPA and HM450 BeadChip

A) Tabulation of 1p/19q status

Formatiert: Zeilenabstand: Doppelt

	1p/19q codeleted (HM450)	1p/19q intact (HM450)
1p/19q codeletion (MLPA)	39	7
1p/19q intact (MLPA)	1	52

Formatiert: Block, Zeilenabstand: Doppelt

Formatiert: Block, Zeilenabstand: Doppelt

Formatiert: Block, Zeilenabstand: Doppelt

Formatiert: Zeilenabstand: Doppelt

B) Cox regression for 1p/19q status

Variable	Hazard Ratio	95% CI	p
1p/19q codeletion, yes vs. no (MLPA)	0.875	0.28 - 2.69	0.817
1p/19q codeletion, yes vs. no (HM450)	0.22	0.06 - 0.79	0.021

Formatiert: Zeilenabstand: Doppelt

Formatiert: Zeilenabstand: Doppelt

CI, confidence interval; HM450, Illumina HumanMethylation450 BeadChip;

Formatiert: Zeilenabstand: Doppelt

MLPA, multiplex ligation-dependent probe assay

Formatiert: Block, Abstand Nach: 0 Pt., Zeilenabstand: Doppelt

Formatiert: Englisch (USA)
Formatiert: Englisch (USA)
Feldfunktion geändert

Table 5: MGMT methylation probability models

Model formula	Cutpoint	Sens.	Spec.	AUC	AIC
logit(y) = 1.3669 + (0.5305 * cg14194875) + (0.5691 * cg12981137)	0.674	0.838	0.807	0.848	86.656
logit(y) = 1.6768 + (0.3427 * cg12434587) + (0.6353 * cg12981137)	0.765	0.709	0.884	0.84	86.686

Formatiert: Zeilenabstand: Doppelt
Formatiert: Zeilenabstand: Doppelt
Formatiert: Zeilenabstand: Doppelt
Formatiert: Schriftart: (Standard) Arial, 12 Pt.

Sens., sensitivity; Spec., specificity; AUC, area under the curve; AIC, An information criterion

Formatiert: Zeilenabstand: Doppelt

SUPPLEMENTARY INFORMATION

Assessing CpG island methylator phenotype, 1p/19q codeletion and *MGMT* promoter methylation from epigenome-wide data in the biomarker cohort of the NOA-04 trial

Benedikt Wiestler, David Capper, Volker Hovestadt, Martin Sill, David TW Jones, Christian Hartmann, Joerg Felsberg, Michael Platten, Wolfgang Feiden, Kathy Keyvani, Stefan M Pfister, Otmar D Wiestler, Richard Meyermann, Guido Reifenberger, Thorsten Pietsch, Andreas von Deimling, Michael Weller, Wolfgang Wick

SUPPLEMENTARY FIGURE 1: TTF by treatment. Kaplan-Meier curves for TTF by treatment arm.

SUPPLEMENTARY FIGURE 2: Overview of the *MGMT* CpG island. Genomic position of the five cg probes significantly associated with *MGMT* methylation, the MSP forward (MSPf) and reverse (MSPr) primers, differentially methylated regions 1 & 2 (DMR1, DMR2) and the region pyrosequenced (PySeq) by Mulholland et al¹ (<http://genome.ucsc.edu>).

SUPPLEMENTARY TABLE 1: *MGMT* promoter methylation assayed by MSP and HM450 by G-CIMP status

A) Non-G-CIMP (n = 20)

	<i>MGMT</i> methylated (HM450)	<i>MGMT</i> unmethylated (HM450)
<i>MGMT</i> methylated (MSP)	6	2
<i>MGMT</i> unmethylated (MSP)	3	9

B) G-CIMP (n = 88)

	<i>MGMT</i> methylated (HM450)	<i>MGMT</i> unmethylated (HM450)
<i>MGMT</i> methylated (MSP)	61	1
<i>MGMT</i> unmethylated (MSP)	23	3

SUPPLEMENTARY TABLE 2: Probes evaluated for correlation with *MGMT* methylation

Probe	p (Log. R.)	p (Bonf. adj.)	AUC (ROC)
cg12981137	6.85E-05	0.00123229	0.82444169
cg14194875	0.00011347	0.00204248	0.8101737
cg12434587	0.00024433	0.00439802	0.77915633
cg02802904	0.00044483	0.00800691	0.76674938
cg00618725	0.0005937	0.01068664	0.75496278
cg12575438	0.03191845	0.57453215	0.66191067
cg26950715	0.85340664	1	0.53970223
cg02330106	0.09707108	1	0.53908189
cg02022136	0.1300395	1	0.60545906
cg23998405	0.11472322	1	0.60297767
cg01341123	0.65465199	1	0.48883375
cg25946389	0.1040175	1	0.5825062
cg16215402	0.84916291	1	0.5353598
cg18026026	0.51003379	1	0.55955335
cg05068430	0.70899511	1	0.48138958
cg19706602	0.27974073	1	0.57816377
cg02941816	0.32090352	1	0.55955335
cg26201213	0.32928739	1	0.45409429

Log. R., logistic regression; Bonf. adj., Bonferroni adjusted; AUC, area under the curve; ROC, receiver operating characteristic

Probes in **bold** are those comprising the model presented by Bady et al.²

SUPPLEMENTARY TABLE 3: *MGMT* status as per MSP and fitted models and Cox regression

A) Model 1: cg14194875 + cg12981137

	<i>MGMT</i> methylated (HM450)	<i>MGMT</i> unmethylated (HM450)	
<i>MGMT</i> methylated (MSP)	52	10	
<i>MGMT</i> unmethylated (MSP)	5	21	
Cox variable	Hazard Ratio	95% CI	p
<i>MGMT</i> M vs. U	0.92	0.39 – 2.14	0.85

B) Model 2: cg12434587 + cg12981137

	<i>MGMT</i> methylated (HM450)	<i>MGMT</i> unmethylated (HM450)	
<i>MGMT</i> methylated (MSP)	44	18	
<i>MGMT</i> unmethylated (MSP)	3	23	
Cox variable	Hazard Ratio	95% CI	p
<i>MGMT</i> M vs. U	0.82	0.37 – 1.81	0.62

M, methylated *MGMT* promoter; U, unmethylated *MGMT* promoter

SUPPLEMENTARY TABLE 4: Overview of clinical and pathological characteristics of all discordant cases (*IDH* / G-CIMP and 1p/19q) as per NOA-04 assessment and HM450 data.

Histology	IDH	G-CIMP	MLPA	HM450 codel	TERT	ATRX
AA	mut	-	intact	intact	wt	expr
AA	mut	+	codel	intact	mut	expr
AO	mut	+	codel	intact	wt	
AA	wt	+	intact	intact		
AA	wt	+		intact	wt	loss
AOA	wt	+	codel	codel		loss
AA	mut	+	codel	intact	wt	loss
AA	mut	+	codel	intact	wt	expr
AO	wt	+	codel	codel		
AOA	wt	+		intact	wt	loss
AA	mut	+	codel	intact	wt	loss
AO	mut	+	intact	codel	mut	expr
AA	wt	+		intact	wt	loss
AO	mut	-	codel	intact	wt	expr
AO	mut	+	codel	intact	wt	expr
AOA	wt	+	codel	codel	mut	expr

AA, anaplastic astrocytoma; AOA, anaplastic oligoastrocytoma; AO, anaplastic oligodendroglioma; mut, mutant; wt, wild type; codel, codeletion; expr, expression

SUPPLEMENTARY TABLE 5: Cox regression for *MGMT* status

Variable	Hazard Ratio	95% CI	p
<i>MGMT</i> , M vs. U (MSP)	0.8	0.39 - 1.64	0.546
<i>MGMT</i> , M vs. U (HM450)	0.19	0.08 - 0.46	< 0.001

CI, confidence interval; HM450, Illumina HumanMethylation450 BeadChip;

MSP, methylation-specific PCR; M, methylated; U, unmethylated

SUPPLEMENTARY TABLE 6: Cox regression analyses for the association of G-CIMP, 1p/19q and *MGMT* status (all per HM450) independent of reference histology and median time to treatment failure (TTF) in molecular subgroups.

A) G-CIMP and reference histology

Variable	Hazard Ratio	95% CI	p
AO vs. AA	0.8	0.37 - 1.76	0.588
AOA vs. AA	0.56	0.28 - 1.12	0.1
G-CIMP, yes vs. no	0.17	0.09 – 0.32	< 0.001

B) 1p/19q and reference histology

Variable	Hazard Ratio	95% CI	P
AO vs. AA	2.22	0.91 - 5.41	0.079
AOA vs. AA	0.82	0.41 - 1.62	0.56
1p/19q codeletion, yes vs. no	0.16	0.06 – 0.39	< 0.001

C) *MGMT* and reference histology

Variable	Hazard Ratio	95% CI	P
AO vs. AA	0.57	0.26 - 1.24	0.157
AOA vs. AA	0.41	0.21 - 1.12	0.076
<i>MGMT</i> , M vs. U	0.18	0.08 – 0.37	< 0.001

CI, confidence interval; AA, anaplastic astrocytoma; AOA, anaplastic oligoastrocytoma; AO, anaplastic oligodendroglioma; M, methylated; U, unmethylated

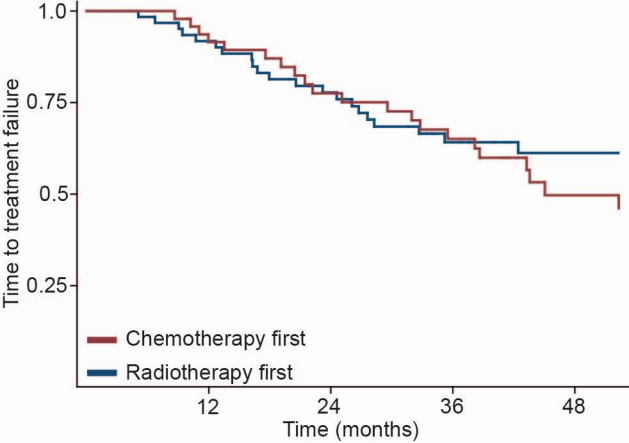
D) Median TTF in molecular subgroups based on G-CIMP and 1p/19q status

Group	Median TTF (95% CI), days
G-CIMP negative (n = 24)	496 (326 – 1080) days
G-CIMP positive, 1p/19q intact (n = 50)	1758 (793 – not reached) days
G-CIMP positive, 1p/19q codeleted (n = 41)	Not reached (1840 – not reached) days

CI, confidence interval

SUPPLEMENTARY REFERENCE

1. Mulholland S, Pearson DM, Hamoudi RA, et al. MGMT CpG island is invariably methylated in adult astrocytic and oligodendroglial tumors with IDH1 or IDH2 mutations. *Int. J. Cancer*. 2012;131(5):1104–1113.
2. Bady P, Sciuscio D, Diserens A-C, et al. MGMT methylation analysis of glioblastoma on the Infinium methylation BeadChip identifies two distinct CpG regions associated with gene silencing and outcome, yielding a prediction model for comparisons across datasets, tumor grades, and CIMP-status. *Acta Neuropathol*. 2012;124(4):547–560.



Scale
chr10:

200 bases

hg19

131,265,200

131,265,300

131,265,400

131,265,500

131,265,600

Your Sequence from Blat Search

cg14194875

cg00618725

cg02802904

MSPr

DMR1

MSPf

DMR2

PySeq

cg12434587

cg12981137

UCSC Genes (RefSeq, GenBank, CCDS, Rfam, tRNAs & Comparative Genomics)

MGMT

100

H3K27Ac Mark (Often Found Near Active Regulatory Elements) on 7 cell lines from ENCODE

Layered H3K27Ac

0

